MESO-SCALE FE MODELLING OF STRUCTURALLY STITCHED PREFORM

V. Koissin, S.V. Lomov, I. Verpoest

Dept. of Metallurgy and Materials Engineering, Katholieke Universiteit Leuven, Kasteelpark Arenberg 44, B–3001 Leuven, Belgium.
E-mail: Vitaly.Koysin@mtm.kuleuven.be

Abstract

This article addresses the finite-element (FE) analysis of a local fibre placement in a stitched fibrous mat. The term "structural" presumes here that the stitching yarn is relatively thick (contrary to a non-structural NCF kniting) and its fibre stiffness is much higher than the matrix stiffness (pure matrix filling so called "openings" — resin-rich zones — around the stitching sites). Simplest 2D FE models are developed; typical carbon-fibre mat, carbon yarn, and epoxy resin properties are used in calculation examples. The results show important influence of the local fibre distribution (caused by the yarn cross-sectional shape, in-plane opening shape, fibre re-orientation around openings, etc.) on the stress-strain fields and homogenized stiffness.

1. Introduction

It is well-known that a non-negligible variability can exist in the micro- and meso-level geometry of a textile composite [1]. Particularly, this is the case for the structurally stitched preforms. The fibre placement is not perfect even in a raw material (NCF or textile fabric). Then, the needles of a knitting device (for NCF's) or a textile process increase this non-uniformity creating openings and zones of affected fibre content. While stitching structurally, Fig. *1*, the fibres are again pushed aside the stitching yarn; a breakage and vertical movement (crimpling) of some fibres can also be induced by the needle [2]. During the forming and out-of-plane compression in a mould, the fibre distribution is changed again. Finally, the micro- and meso-structure of a composite part can differ very much from that of the raw fabric.
Variability of the internal structure is also characterized by its strong randomization caused by a random nesting of layers, random overlap of the "structural" and "non-structural" piercing patterns and openings (for NCF's), wide distribution of the opening dimensions, etc.
In FE analysis, such complex structure is inevitably idealized is certain extend. This brings up a question about the degree of idealization: to model or not to model the "structural" and "non-structural" openings (with which shape? accounting for a possible overlap?), stitching yarn (which shape of the loop path and cross-section?), nesting, etc. The present study aims at investigation of a typical influence of several local modelling features on the stress distribution in a stitched fibrous mat and its homogenized stiffness. Results of FE modelling are presented and discussed, although the analysis is based on a limited evidence.

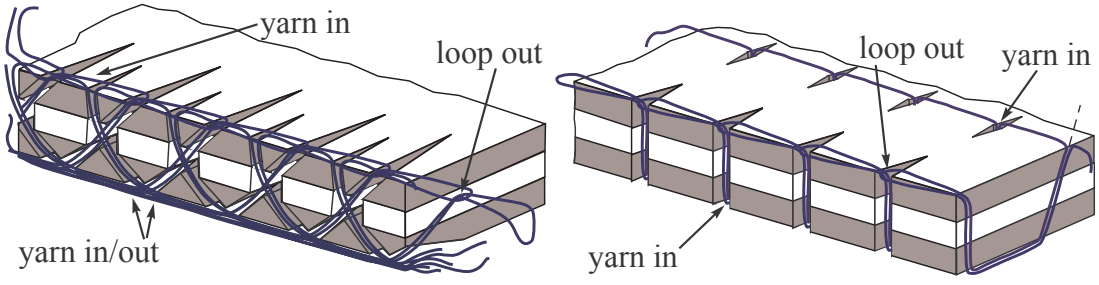

Fig. 1. Curved needle (left) and dual needle (right) stitching methods.

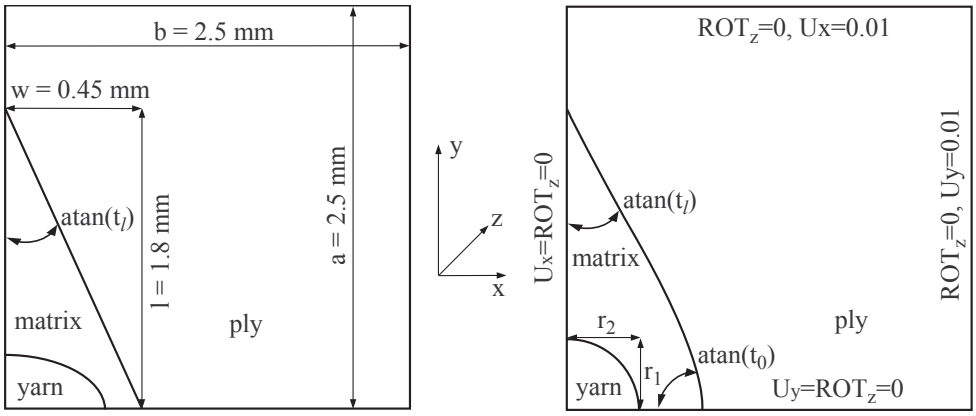

Fig. 2. Geometrical model for the cases of elliptic yarn cross-section and rhomb opening (left) or circular yarn cross-section and 'realistic' opening (right).

2. Modelling

2.1. Modelling approach

A stitched laminate has several structural levels: 1) micro-level as a local fibre arrangement, 2) meso-level as a textile structure of the layers and geometry of the stitching loop binding them together, 3) macro-level as configuration of a structural part or a test sample. This study is focused on the micro- and meso-levels; the following details are considered:

- Cross-sectional shape of a structural stitching yarn. The experimental data, [2], reveals that the shape can be very randomized. Also, the cross-sections of two neighboring yarns often interpenetrate each other in the through-the-thickness path of a stitching loop. In this paper, an idealized case is studied, when two yarns are presented as a single yarn having elliptic cross-section. The ratio of its major and minor axes is varied, Fig. *2*, and influence of this variation on the stress distribution is detected.

  The multifilament stitching yarns can also have a non-uniform fibre distribution in the cross-section, [3]. The fibre content is usually decreased towards the yarn edge; however, the maximal content can appear somewhere in between the centre and the edge. This effect is not addressed here, since it has already been studied earlier, [4], and its important influence on the stress maximums has been revealed.

- It is also interesting to access significance of the stitching yarn modelling in an FE analysis: a stitching loop configuration is quite complex, [5], and if it is possible to have reasonable estimation of the composite properties without stitching included (as it is done in [6]), then an FE meshing can be much easier and the computational cost lower.

- In-plane shape of the openings. Similarly to a stitching yarn, their shapes and dimensions are very randomized in a real stitched preform [2]. When modelling, it is usually accepted that the openings are equal in size, diamond-shaped in the preform plane, and perfectly oriented along the global fibre orientation in the ply. In the present study, yet idealized (with averaged dimensions) but more general configuration is considered, which includes the rhomb shape as one of the limit cases, Fig. *2*.

- local fibre re-orientation sideways the opening, Fig. *3*(left).

A simple 2D model of one layer is used to explore the listed features; thus, a laminate structure is not modelled. This approach does not allow to account for a complex interaction (nesting, etc.) as between different plies as well as between openings in these plies. In reality the layers

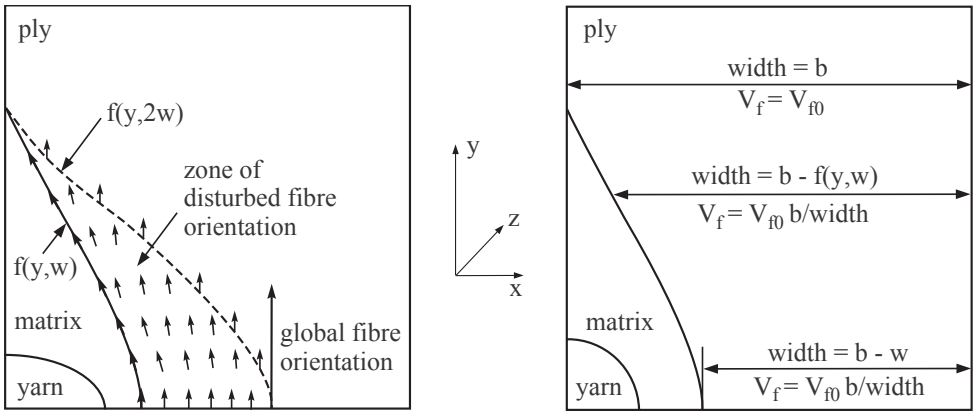

Fig. 3. Local fibre deviation around opening (left) and local fibre compaction between the openings (right). Meaning of the function $f(y, w)$ is explained in Subsection 2.2.

can heavily be nested and even deplaned by the out-of-plane compression when consolidating the laminate. Actual 3D shape of the stitching yarn (twist, varying cross-section, loop path, etc.) is also not modelled here, although it can be important for the stress assessment in zones between the plies and at the surface plies (and of course for the out-of-plane stiffness).
Randomization of the internal structure is not taken into account; it is obvious that there is no possibility to account for all randomized features of a real composite. However, the "averaged" model of one ply is an important simplification allowing for simple and easy-interpretable qualitative results. The physical meaning of this model can be the stress-strain state near the the midplane of a relatively thick UD fibre layer of a stitched laminate.
It is also accepted in the numerical modelling that the local fibre orientation is symmetric with respect to x-y axes, Fig. *3*(left). Another assumption deals with a local fibre densification between the openings. There is no experimental data on this subject but it is obvious that this effect can exist in a real stitched fabric as illustrated in Fig. *3*(right). The experimental data, [2], reveal also that the fibre volume fraction can locally decrease towards the edge of the opening. In this study, it is accepted that the fibres are uniformly distributed in the ply domain.

2.2. Materials

Basic properties of the materials used in the present study are listed in Table *1*; the materials are considered as linear-elastic. The ply material is a typical carbon/epoxy composite. Thick carbon yarn is inserted across the ply with 5×5 mm piercing pattern, Figs. *2* and *3*. This stitching creates openings with the average length of 3.6 mm and average width of 0.9 mm, Fig. *2*(left). Radius of the equivalent circular yarn cross-section is calculated as

$$r_0 = \sqrt{2T/\pi\rho K} \quad [mm], \tag{1}$$

where K is the packing coefficient (here, 0.58), T is the yarn linear density (67 tex), ρ is the fibre material density (1760 kg/m^3). Factor 2 is used, since two yarns are modelled together. For a given ratio between the minor and major axes of the elliptic cross-section, the area calculated using this radius is preserved to keep the fibre volume fraction of 58% inside the yarn.
The same average fibre volume fraction is kept for the whole model in all calculations (without taking into account the yarn fibres). For example, the volume of fibres is decreased by the volume of the opening (rhomb 0.9x3.6 mm in the simplest case). For 5×5 mm unit cell, this increases the average fibre volume fraction up to 62%. Homogenized properties of impregnated fibres are calculated using the rule of mixture formulae (assuming UD fibre arrangement both in the ply and in the stitching yarn). If an uneven fibre distribution would be modelled in the ply, Fig. *3*(right), the rule of mixture would be applied separately at each desired point.

Table 1. Properties of the composite constituents

	material	fibre ∅, μm	density, kg/m^3	Young's modulus, GPa	Poisson's ratio *
ply	Tenax HTA 5231	5	1800	290*/14**	0.236*/0.011**
yarn	Tenax IMS 5131	7	1760	238*/14**	0.230*/0.014**
matrix	Cycom 977-2	7	1310	3.52	0.30

* longitudinal, ** transversal (theoretically estimated for the Poisson's ratios)

The edge of the opening is determined by the elastic line equation

$$f(y,w) = \big(2w + l(t_0 + t_l)\big)(y/l)^3 - \big(3w + l(2t_0 + t_l)\big)(y/l)^2 + t_0 y + w, \qquad (2)$$

where w and l are half-width and half-length of the opening, Fig. *2*. The parameters t_0 and $t_l{=}{-}w/l$ define inclination of the curve at $y{=}0$ and $y{=}l$. The parameter t_l is kept constant, while t_0 is varied between t_l and 0. The latter case, Fig. *2*(right), gives the opening with refined configuration, which has no geometrical stress concentrator at ($y{=}0$, $x{=}w$).
When modelling the local fibre deviation, this effect is assumed to be confined between the curves $f(y,w)$ and $f(y,2w)$. Then, the additional angle at a point (x_0, y_0) is calculated as

$$\triangle\alpha = -\arctan\big(f'_y(y_0,w)(1-r)\big), \quad r = \big(x_0 - f(y_0,w)\big)/\big(f(y_0,2w) - f(y_0,w)\big). \qquad (3)$$

2.3. FE model

Two-dimensional FE model is meshed using 3- or 4-node shell elements. First, three surfaces are created for the ply, yarn, and matrix domains (in several cases, the yarn domain is omitted to model the case without stitching). Then, the surfaces are automatically meshed using 3-node elements with the condition of a coincident number of nodes at a boundary between neighbouring surfaces. The average element size is preserved to be equal in all material domains. Finally, the elements are automatically substituted for 4-node ones, in oder to decrease the number of elements and improve the mesh. If the uneven fibre orientation is modelled, the local coordinate systems of the elements are rotated around z-axis according to Eq. (3).
Due to the symmetry, only a quarter of the unit cell structure is meshed. Typical model geometry with the imposed boundary conditions is shown in Fig. *2*(right). Uniaxial tensile load is applied separately using a prescribed displacement: 1) along or 2) across the overall fibre orientation in the ply; this orientation coincides with y-axis in Figs. *2* and *3*.
As a reference, the model of 'intact' (no stitching yarn, no opening, evenly distributed UD fibres) composite is also built and tested numerically.

3. Results and discussion

Results of the linear-elastic analysis are compared according to three parameters: 1) maximal stress in the load direction, 2) position of this maximum, and 3) homogenized stiffness in the load direction. The results are presented in Figs. *4–9* being normalized against corresponding values obtained for the intact composite (without yarn, opening, and fibre distortion). Parameter $k{=}r_1/r_2$ is the aspect ratio between y and x axes of the elliptic yarn cross-section, Fig. *2*(right); k is varied from 1/3 to 3. Case $k{=}0$ virtually presents the model with opening but without yarn.

3.1. Variable yarn cross-section

As can be seen in Figs. *4*(left) and *5*, under loading across the ply fibres, the maximal stress σ_x is sensitive to the yarn cross-section shape only if the yarn edge approaches the opening

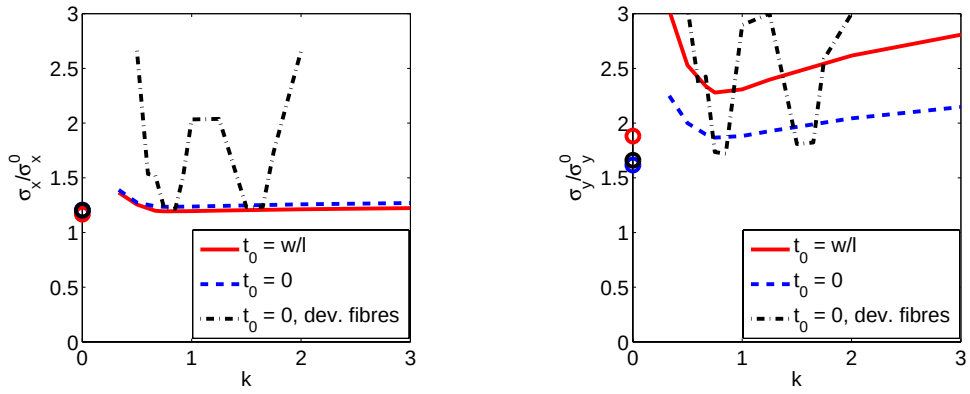

Fig. 4. Normalized maximal stress σ_x under tension in x-direction (left) and σ_y under tension in y-direction (right). Cases $t_0{=}w/l$ and $t_0{=}0$ correspond to the shapes of the opening shown in Figs. 2(left) and 2(right), respectively. "Dev. fibres" designates the model with locally deviated fibre orientation, Fig. 3(left). Normalized against values for unstitched UD composite.

edge (this occurs when the cross-section is very elongated in x-direction). For example, case $k{=}1/3$ gives the stress rise of 36% (17% if compare with the value at $k{=}0$). For other cases, $k{=}1/2$, when the yarn and ply materials are separated with a relatively wide matrix domain, the maximal stress does not differ very much from that obtained for the model without yarn ($k{=}0$) or even for the intact composite. However, it is important that the maximal stress changes its position somewhere between the cases $k{=}1/2$ and $k{=}3/4$; the maximum migrates from the yarn tip ($x{=}r_2$, $y{=}0$) to the opening corner ($x{=}0$, $y{=}l$). It is interesting that the model without yarn shows the maximum also near ($x{=}0$, $y{=}l$). Despite this migration, the stress value changes monotonically. However, for another material combination, it should be suggested that the shift of the maximal stresses position can be accompanied by a change in their magnitude.
Under loading across the ply fibres, Figs. *4*(right) and *6*, the migration is not observed; the maximum of σ_y always appears near the point ($x{=}w$, $y{=}0$). The stress rise magnitude is more pronounced than for the transversal loading; the magnitude increases by 300% in the case $k{=}1/3$ (50% if compare with the case $k{=}0$). Such different sensitivity to the loading direction is obviously due to the large difference between the fibre and matrix stiffnesses, which is especially manifested when the model is loaded along the fibres. As a result, the stress concentration appears at the interface between two kinds of materials (pure resin and impregnated fibres) with high property mismatch. When the yarn cross-section approaches the circular shape, the maximal stress decreased monotonically. This is obviously because the maximum appears near the opening corner and is not influenced very much by the yarn if it is placed far from this point. However, it is worth to note that further increase of k rises the stress magnitude again; for example, considerable stress rise is detected for $k{=}3$, when the yarn cross-section is elongated in y-direction; the reason of this phenomena is not yet understood by the authors.
As for the homogenized stiffness, as could be expected, the yarn cross-sectional shape shows negligibly small influence (less than 2%) on this parameter in both directions, Fig. *7*.

3.2. Variable opening shape

The overall view of the stress fields is very similar for the cases with straight, Fig. *2*(left), and curved, Fig. *2*(right), opening edge. Positions of the stress maximums are also the same. However, the curved shape results in considerably lower maximum of σ_y as can be seen in Fig. *4*(right). Simultaneously, maximum of σ_y slightly increases, Fig. *4*(left). The maximal difference between σ_y in the cases of straight or curved opening edge consists 35% at $k{=}1/3$; it can be expected that a more elongated elliptic profile gives even higher difference.

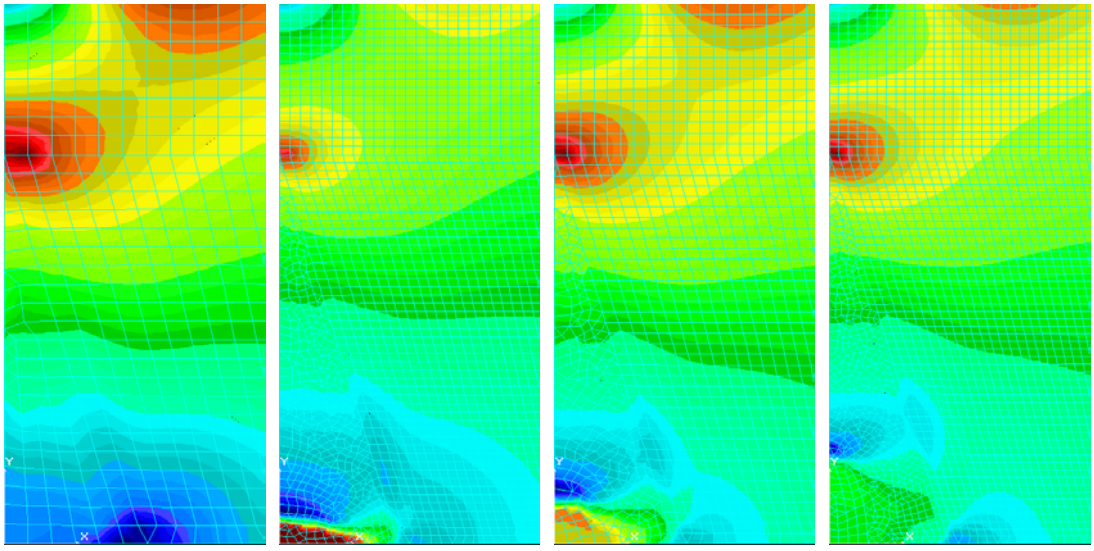

(a) k=0 (no yarn) (b) k=1/2 (c) k=1 (d) k=2

Fig. 5. Stress σ_x under tension in x-direction for different yarn cross-section profiles. Detail. Case of straight edge of the opening, without local fibre re-orientation.

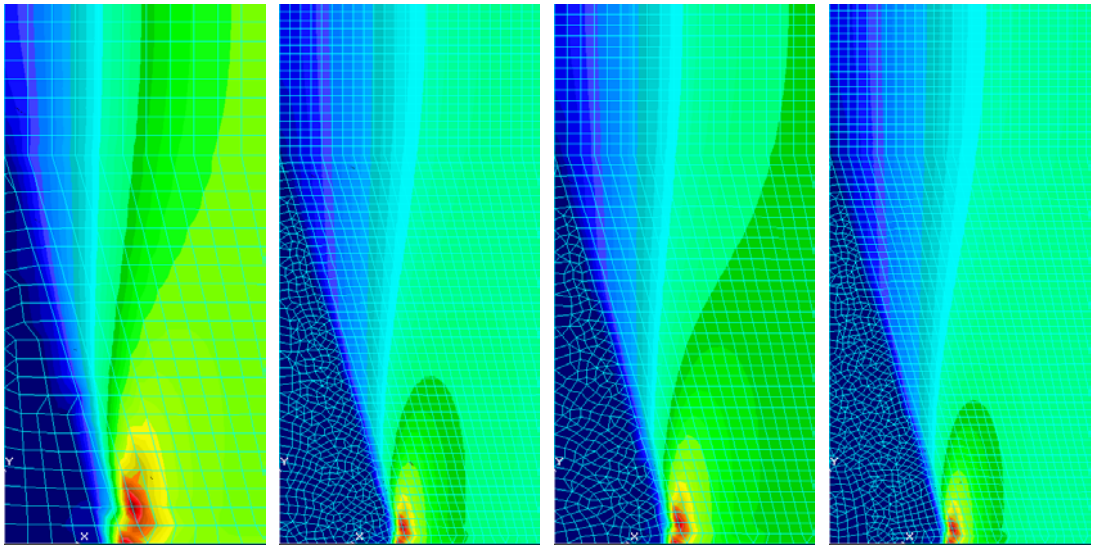

(a) k=0 (no yarn) (b) k=1/2 (c) k=1 (d) k=2

Fig. 6. Stress σ_y under tension in y-direction for different yarn cross-section profiles. Detail. Case of straight edge of the opening, without local fibre re-orientation.

It is seen that the opening shape is not important for the assessment of the homogenized stiffness, Fig. *7*; this conclusion could be derived even without an FE analysis.

3.3. Disturbed fibre orientation sideways openings

Accounting for a local deviation of fibres near the opening results in very interesting phenomena in both load cases (along and across the fibres). This phenomena occurs approximately when $k<3/4$ or $0.85<k<1.5$ or $k>1.65$. First, as can be seen in Figs. *8* and *9*, the maximal stress position moves from the corner points ($x=0$, $y=l$ for σ_x or $x>w$, $y=0$ for σ_y) to an intermediate position near the outer boundary of the fibre deviation zone (this position is almost the same both for σ_x and σ_y). This migration is accompanied by a prominent increase of the maximal stress

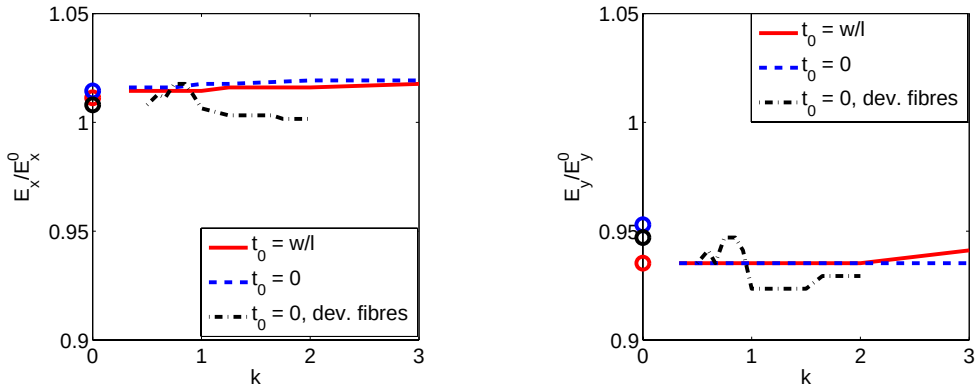

Fig. 7. Normalized homogenized stiffness E_x under tension in x-direction (left) and E_y under tension in y-direction (right). Cases $t_0{=}w/l$ and $t_0{=}0$ correspond to the shapes of the opening shown in Fig. 2. "Dev. fibres" refers to a locally deviated fibre orientation, Fig. 3(left). Normalized against values for unstitched UD composite ($E_x^0{=}6.22$ GPa, $E_y^0{=}170$ GPa).

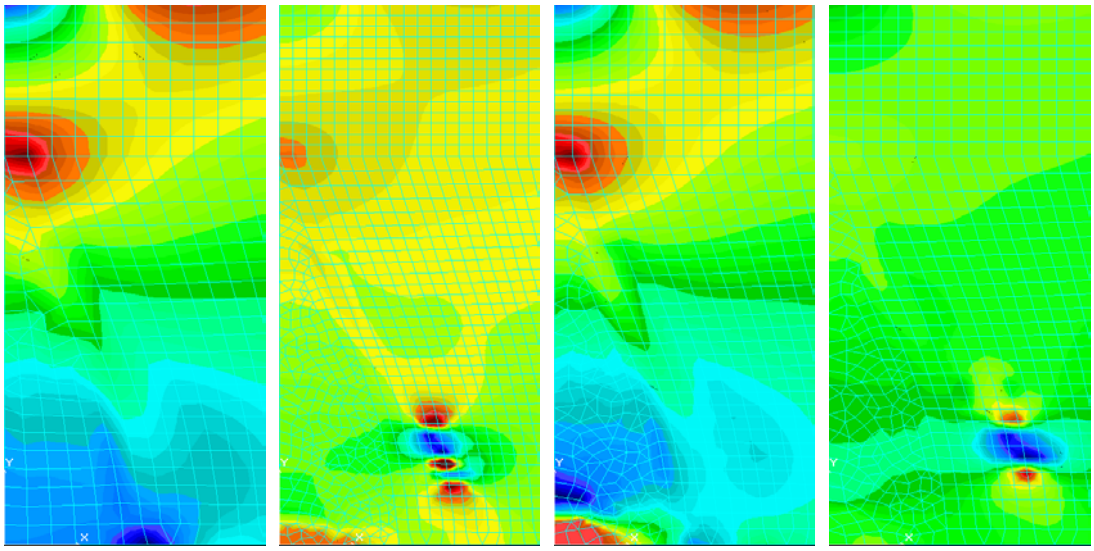

(a) k=0 (no yarn) (b) k=1/2 (c) k=3/4 (d) k=1

Fig. 8. Stress σ_x under tension in x-direction for different yarn cross-section profiles. Detail. Case of curved edge of the opening, with local fibre re-orientation.

magnitudes as shown in Fig. *4*; the stress growth exceeds 100%, if compare with the values at $k{=}1$. Reason of this phenomena is not yet completely clear for the authors.
As in the previous cases, the local fibre re-orientation has a small influence on the homogenized stiffness, Fig. *7*; this is obviously due to a relatively small width and large length of the opening that results in a small fibre deviation. For wider openings the effect can be more pronounced but no considerable influence should be expected in any case.

4. Conclusions

The presented study deals with local fibre placement in stitched composites and its influence on the stress distribution and homogenized stiffness. The main results can be outlined as

- the local geometry of the openings, stitching yarn cross-sections, and local deviation of fibres from their global orientation are not important for calculation of the homogenized in-plane stiffness; presence of openings is also not important in this case. The difference is within 3% that is much less than the allowable engineering precision;

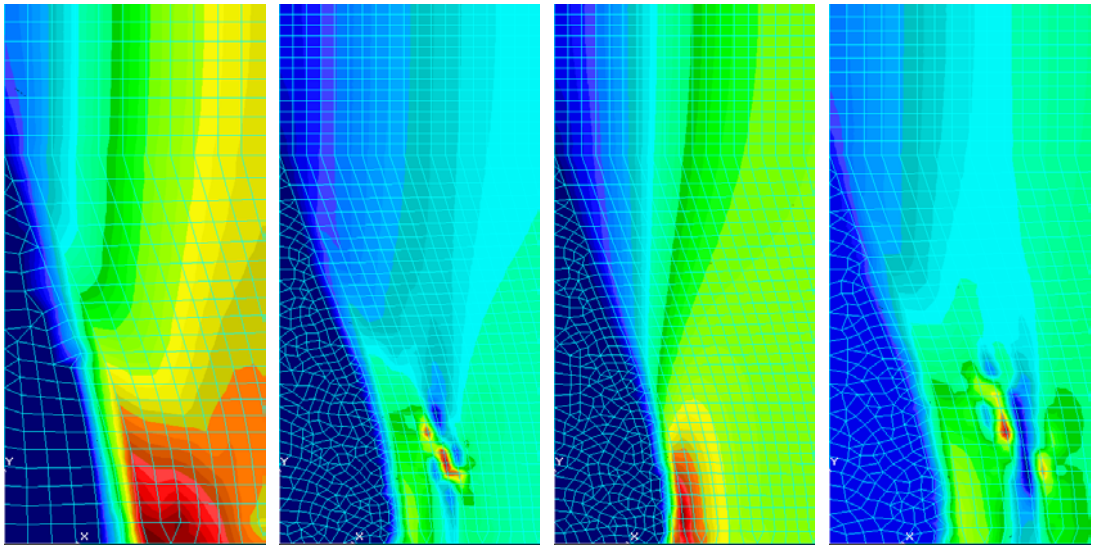

(a) k=0 (no yarn) (b) k=1/2 (c) k=3/4 (d) k=1

Fig. 9. Stress σ_y under tension in y-direction for different yarn cross-section profiles. Detail. Case of curved edge of the opening, with local fibre re-orientation.

- the stress-strain fields can be very sensitive to the local geometry, which can play the role of a stress concentrator. In the present study dealing with typical carbon-epoxy composite, a change of the yarn cross-section or geometry of the opening edge can result in a 35% growth of the maximal stress magnitude. When the local fibre re-orientation is accounted for, the maximal stress growth about 100% is obtained;
- therefore, presence of the stitching yarn and specifics of its modeling can be very important for a correct computation of the local stress-strain fields in a stitched fibrous mat, especially under loading along the global fibre orientation. Shape of the opening and a local fibre re-orientation near it can also be very important for the strength calculations.

5. Acknowledgments

This study was done within the I-TOOL (“Integrated Tool for Simulation of Textile Composites”) project founded by the European Commission.

References

1. Åström, B.T. Manufacturing of polymer composites, Chapman & Hall, 1997.
2. V.Koissin, A.Ruopp, S.V.Lomov, I.Verpoest, V.Witzel, and K.Drechsler. Internal structure of structurally stitched NCF preform. *Proc. of 12th European Conference on Composite Materials (ECCM-12), Biarritz, France, August 29 — September 1, 2006* CD-edition.
3. S.A.Grishanov, S.V.Lomov, T.Cassidy, and R.J.Harwood. The simulation of the geometry of two-component yarns. Part II: Fibre distribution in the yarn cross-section, *Journal of the Textile Institute*, **88**(4): 352–372 (1997).
4. V.Koissin, D.S.Ivanov, S.V.Lomov, and I.Verpoest. Fibre distribution inside yarns of textile composite: geometrical and FE modelling. *Proc. of 8th Int. Conference on Textile Composites (TexComp-8), Nottingham, UK, October 16–18, 2006*, CD edition.
5. V.Koissin, S.V.Lomov, and I.Verpoest. Internal geometry of structurally stitched ncf preforms . *Proc. of 16th Int. Conference on Composite Materials (ICCM-16), Kyoto, Japan, July 8th–13, 2007*, CD edition.
6. H.Heß, Y.C.Roth, and N.Himmel. Elastic constants estimation of stitched NCF CFRP laminates based on a finite element unit-cell model, *Composites Science and Technology*, **67**(6): 1081–1095 (2007).